

Subshell coupling effects in L -shell ionization of gold by proton impact

László Sarkadi* and Takeshi Mukoyama

Institute for Chemical Research, Kyoto University, Kyoto, 606 Japan

(Received 29 September 1987)

The effect of subshell couplings on L -shell ionization cross sections for protons on gold has been estimated in the energy range 0.15–3 MeV. The applied model treats the couplings dynamically solving a set of coupled differential equations which govern the time evolution of the L -substate amplitudes. The effect has been found to be particularly large for the L_2 subshell, reaching 40% at low collision energies. The results of the calculations were used to correct the cross-section values obtained by Chen and Crasemann in the plane-wave Born approximation with use of Dirac-Hartree-Slater wave functions. The combined theory reproduces the structure observed recently by Jitschin *et al.* in the energy dependence of the L_2 - and L_3 -shell cross-section ratio.

For a long time the atomic inner-shell ionization by light ions has been the subject of many theoretical and experimental investigations. One of the most frequently used ionization theories is the plane-wave Born approximation¹ (PWBA). To increase its accuracy in the description of the experimental data, various effects, such as the deflection of the projectile in the Coulomb field of the target nucleus, the distortion of the state of the electron to be ionized (increased binding energy, polarization of the charge cloud), and the electronic relativistic effects, have been incorporated into the theory.²⁻⁵ Further improvements have been obtained employing more realistic than hydrogenlike wave functions.⁶⁻⁹

For degenerate or nearly degenerate subshells, the consideration of the dynamical couplings between the subshell ionization amplitudes is necessary. The subshell couplings take place through a secondary (or multiple) interaction between the projectile and the target electrons, and can be considered as higher-order processes. Therefore, the coupling effect increases with increase of the atomic number of the projectile Z_1 . We have found order-of-magnitude deviation from the first-order theories for L -subshell ionization by heavy-ion impact or heavy target.¹⁰⁻¹⁵ However, in the case of heavy-ion impact, only gross features are studied because of other disturbing effects: the screening effect due to the projectile electrons¹⁶ and the large probability of charge-transfer processes. For proton impact such disturbing effects do not exist, but the subshell couplings are expected to be weak.

In order to study the subshell coupling effects the L_2 - and L_3 -shell ionization cross-section ratio is an especially suitable quantity for the following reasons. First, the ratios of cross sections can be measured with much higher accuracy than absolute cross sections. Second, the L_2 -to- L_3 ratio is a smooth function as a function of the projectile energy, because both states are $2p$ states with difference in the binding energy only (exactly speaking, there is a small difference in the radial wave functions due to the relativistic effects).

Figure 1 shows the comparison of theoretical and experimental L_2 -to- L_3 ratios for protons on gold target in the energy range of 0.15–3 MeV. The effect of the relativity

and of the choice of the wave functions is demonstrated by comparing the PWBA calculations with screened hydrogenic nonrelativistic¹ (PWBA-SH) and Dirac-Hartree-Slater⁹ (RPWBA-DHS) wave functions. The latter model corrected for the Coulomb deflection and binding effects (RPWBA-DHS-BC) is also plotted as the most complete description of L -shell ionization by the first-order theories. The experimental data are taken from Jitschin, Kaschuba, Nippler, and Lutz.¹⁷ It can be seen from Fig. 1 that the RPWBA-DHS-BC is in satisfactory agreement with experiment and this is the reason that the contribution of the higher-order terms of the Born series to the subshell cross sections has been thought to be negligible.¹²

However, it should be noted that the experimental L -subshell ionization cross sections have been converted from the measured x-ray production cross sections¹⁸ and sensitively depend on fluorescence yields and Coster-

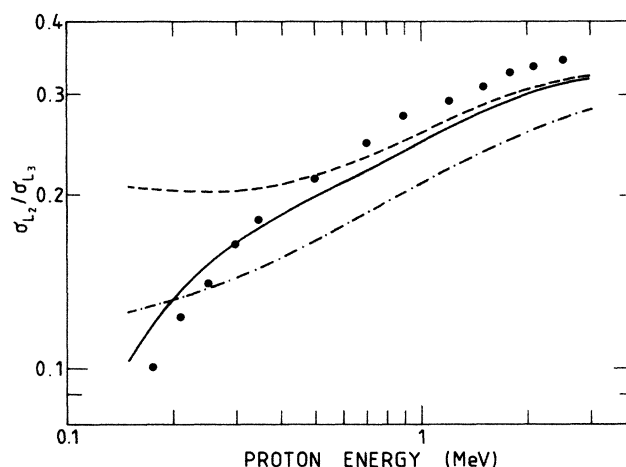


FIG. 1. L_2 -to- L_3 -subshell cross-section ratios for ionization of gold by protons. Theories: dashed-dotted curve, PWBA-SH (Ref. 1); dashed curve, RPWBA-DHS (Ref. 9); solid curve, RPWBA-DHS-BC (Ref. 9). The experimental data (solid circles) are from Jitschin *et al.* (Ref. 17).

Kronig factors. Recently Jitschin *et al.*¹⁹ measured the vacancy decay parameters for the L subshells of gold using synchrotron radiations and found significant deviations from the published values.²⁰ Using the new set of atomic parameters, they reevaluated their earlier measurements.¹⁷ The revised values for the L_2 -to- L_3 ratio are reproduced in Fig. 2 (solid circles).

From comparison of Figs. 1 and 2, it is clear that the new decay parameters have a considerable effect on the experimental cross-section ratios. The agreement with the RPWBA-DHS-BC theory (dashed curve) becomes worse both in shape and magnitude. At the same time, a new interesting feature, a fluttering at about 0.4 MeV, appears in the energy dependence of the reevaluated data. The reason for the absence of this structure in the old data can be ascribed to the large f_{12} Coster-Kronig transition probability adopted above:²⁰ The old value is 0.14, while the new one is 0.047.

The insufficiency of the first-order theories for the reevaluated data and particularly the appearance of the structure in the energy dependence have motivated us to estimate the coupling effects in L -shell ionization by proton impact. In the present work, we apply the coupled-states model, whose details can be found elsewhere.^{13,21,22} We use the impact-parameter approach in the semiclassical approximation (SCA) and consider only terms containing L -subshell amplitudes. Then we have one equation for each transition into unoccupied final states with amplitudes $a_f(t)$ (in atomic units):

$$\frac{da_f}{dt} = -i \sum_{n_L} \mathcal{V}_{fn_L} a_{n_L}, \quad (1)$$

and eight coupled equations for the L substate amplitudes

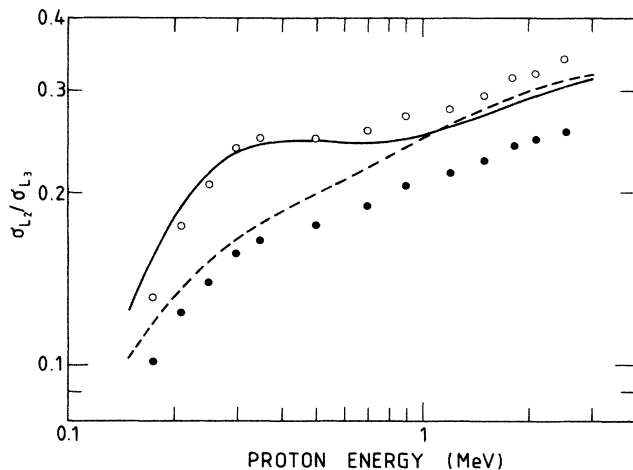


FIG. 2. L_2 -to- L_3 -subshell cross-section ratios for ionization of gold by protons. The dashed curve denotes the RPWBA-DHA-BC theory (Ref. 9); the solid curve represents the same theory but with inclusion of the subshell coupling effects. The experimental points are from reevaluation of the x-ray data of Jitschin *et al.* (Ref. 17) with use of atomic decay (Ref. 19) parameters obtained by synchrotron-radiation excitation (Ref. 19) (solid circles), and applying decay parameters taken from theory (Refs. 26 and 27) (open circles).

$a_{n_L}(t)$:

$$\frac{da_{n_L}}{dt} = - \sum_{n'_L} \mathcal{V}_{n_L n'_L} a_{n'_L}. \quad (2)$$

Here n_L represents a set of quantum numbers l, j , and m_j of the eight L substates. The $\mathcal{V}_{mk}(t)$ matrix elements for the projectile-target-electron interaction are defined as

$$\begin{aligned} \mathcal{V}_{mk}(t) &= V_{mk}(t) \exp(i\omega_{mk}t), \\ V_{mk}(t) &= \int d\mathbf{r} \psi_m^*(\mathbf{r}) \frac{-Z_1}{|\mathbf{r} - \mathbf{R}(t, b)|} \psi_k(\mathbf{r}), \\ \omega_{mk} &= E_m - E_k, \end{aligned} \quad (3)$$

where R is the internuclear vector, b is the impact parameter, and $\psi_j(r)$ and E_j are the one-electron energy eigenstates and eigenvalues of the unperturbed target atom. The cross section for vacancy production in a state labeled by i is given by²³

$$\sigma_i = 2\pi \int_0^\infty db b \sum_f |a_f(t = +\infty)|^2. \quad (4)$$

Here the a_f amplitudes are obtained by integration of Eq. (1) using the same set of a_{n_L} amplitudes for every final state at a fixed impact parameter. The $a_{n_L}(t)$ functions are obtained by solving Eq. (2) with the initial condition $a_n(t = -\infty) = \delta_{n_L i}$.

For simplicity, only some representative, dominant transitions with a limited number of final states are chosen to characterize the ionization process. In low-velocity collisions, where the coupling effects are expected to be large, the dominant transitions are those which take place with minimum energy transfer. For a similar reason the angular momentum of the ionized electrons in the final state is restricted to $l_f = 0$ and 1. The higher-order effects estimated in this are incorporated into a first-order theory as a *correction factor* which is defined for the i th subshell by

$$c_i = \sigma_i^{(c)} / \sigma_i^{(1)}. \quad (5)$$

Here $\sigma_i^{(1)}$ and $\sigma_i^{(c)}$ denote the subshell ionization cross sections corresponding to the first-order theory [i.e., solution of Eq. (1) with $a_{n_L}(t) = \delta_{n_L i}$] and to the coupled-states theory [Eqs. (1) and (2)], respectively. The prime indicates that the cross sections are calculated with a limited number of final states as described above. We assume that the subshell coupling effects do not differ much for transitions with larger values of energy and angular momentum transfer and use C_i , defined by Eq. (5), to correct cross sections obtained from the first-order theory (e.g., PWBA):

$$\sigma_i^{(c)} \approx C_i \sigma_i^{(1)}. \quad (6)$$

It is also assumed that the subshell coupling processes are mainly sensitive to the symmetry of the states involved²⁴ but not to the details of the wave functions. The bound-bound and bound-free matrix elements of the projectile-electron interaction [Eq. (3)] are evaluated with the screened nonrelativistic hydrogenic wave functions.²¹ Since the Coulomb deflection effect is large at low collision energies, the hyperbolic Kepler orbit is used for the projectile path.²¹ The binding effect is automatically in-

cluded in the solution of the coupled equations^{22,25} and no correction is needed for $\sigma_i^{(c)}$. This is not the case for the first-order cross section $\sigma_i^{(1)}$, where we follow the procedure of Brandt and Lapicki,³ i.e., modify the binding energy of the initial state

$$E_i \rightarrow E_i + \Delta E_i ,$$

with

$$\Delta E_i = V_{ii}(b, t=0) .$$

The time $t=0$ corresponds to the distance of the closest approach of the two nuclei at a given impact parameter.

The obtained correction factors for the three subshells are listed in Table I. The subshell coupling effect is surprisingly large for the L_2 subshell, almost 40% at low proton energies. Using the correction factors we have modified the RPWBA-DHS-BC cross sections according to Eq. (6), and plotted the L_2 -to- L_3 ratio in Fig. 2 (solid curve). Though there still remains a disagreement in absolute scale, considerable improvement can be observed in description of the shape of the energy dependence. The present model gives account of the curious structure, correctly reproducing its position, but slightly overestimating its extent.

One can hardly attribute the remaining deviations between the theory and experiment, at an average 35%, to any known effect influencing the theoretical ionization cross sections. Particularly the deviation at large proton energies (20%) is unexplainable from the theoretical view point because all the corrections (Coulomb deflection, bind, subshell coupling effects) rapidly decrease with increasing collisional energy and the RPWBA-DHS cross sections have been calculated with realistic atomic wave functions.

Since the experimental data are sensitive to the atomic decay parameters adopted, it is interesting to use another set of atomic parameters to find the reason of the discrepancy. For this purpose, we used *theoretical* decay parameters in evaluation of the same x-ray experimental data, and took the fluorescence yields and Coster-Kronig rates from Chen, Crasemann, and Mark²⁶ and the x-ray emission rates from Scofield.²⁷ The data set of Chen *et*

TABLE I. Correction factors for inclusion of the subshell coupling effects in L -shell ionization of gold by protons of energy E_1 (in MeV).

E_1	c_{L_1}	c_{L_2}	c_{L_3}
0.15	0.99	1.25	1.03
0.20	0.96	1.38	1.00
0.25	0.93	1.39	0.98
0.30	0.90	1.37	0.96
0.40	0.86	1.25	0.95
0.60	0.84	1.09	0.94
0.80	0.85	1.00	0.94
1.00	0.85	0.96	0.95
1.50	0.91	0.94	0.96
2.00	0.94	0.95	0.97
3.00	0.96	0.97	0.98

TABLE II. Fluorescence yields and Coster-Kronig factors for gold.

	Krause (Ref. 20)	Jitschin (Ref. 19)	Chen (Ref. 26)	Present
w_1	0.107(16)	0.135(9)	0.076	0.100
w_2	0.334(17)	0.401(20)	0.355	0.390
w_3	0.320(10)	0.320(10) ^a	0.310	0.320 ^a
f_{12}	0.140(14)	0.047(10)	0.074	0.030
f_{13}	0.530(27)	0.590(20)	0.704	0.700
f_{23}	0.122(18)	0.100(9)	0.129	0.100

^aNormalized to the value given by Krause (Ref. 20).

*al.*²⁶ is interesting due to the fact that their f_{12} Coster-Kronig rate is 0.074, i.e., a low value supporting the result of the synchrotron radiation measurement. We used the proton-induced L x-ray intensity ratios (L_{γ_1}/L_a and $L_{\gamma_{2,3,6}}/L_a$) given by Jitschin *et al.*¹⁷ in tabulated form and derived the new subshell cross-section ratios. The results are shown in Fig. 2 by open circles. The agreement with the present calculations is quite good. We regard this remarkable agreement as a great success in the theoretical description of L -shell ionization: The complete collision process including both ionization and decay of the atom is well accounted by the theory. Furthermore, it is clear that the subshell couplings are relatively strong for proton impact and cannot be neglected in cross-section calculations.

Finally, we attempted to get an even better agreement between theory and experiment by treating the fluorescence yields and Coster-Kronig transition probabilities as free parameters and by adjusting them in a small extent. The best parameters thus obtained are listed in Table II together with the values of Krause,²⁰ Jitschin, Materlik, Werner, and Funke¹⁹ and Chen, Crasemann, and Mark²⁶

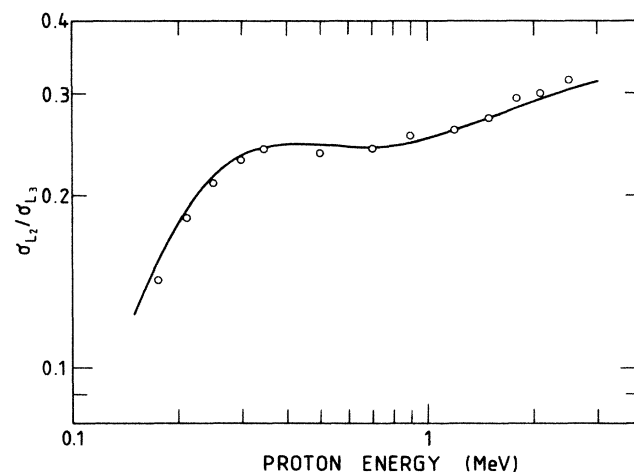


FIG. 3. L_2 -to- L_3 -subshell cross-section ratios for ionization of gold by protons. The solid curve is a repetition from Fig. 2. The open circles represent a fit to the curve obtained with use of optimized values of fluorescence yields and Coster-Kronig factors converting the x-ray data of Jitschin *et al.* (Ref. 17) into subshell ionization cross sections.

(corresponding to Figs. 1 and 2) and the fitted cross-section ratios are plotted in Fig. 3. The agreement is excellent. We note that this result is obtained with decay parameters which seem to be realistic from comparison with other parameter sets in Table II. However, we do not regard these values as recommended ones, because the analysis of the L_1 -to- L_2 ratio would be necessary, and also we do not believe that the experiment and theory are without errors.

In conclusion, we have strong evidence for the existence

of the subshell couplings in *L*-shell ionization of gold by proton impact. The revelation of the coupling effects hidden in the *L* x-ray production cross sections, however, critically depends on the atomic decay parameters used to deduce the subshell ionization cross sections from the raw experimental data. Further studies are needed especially in this context.

This paper is based on work supported by the Japan Society for Promotion of Science.

*Permanent address: Institute of Nuclear Research, Hungarian Academy of Sciences (ATOMKI), H-4001 Debrecen, Postfach 51, Hungary.

- ¹E. Merzbacher and H. W. Lewis, *Handb. Phys.* **34**, 166 (1958).
- ²W. Brandt and G. Lapicki, *Phys. Rev. A* **10**, 474 (1974).
- ³W. Brandt and G. Lapicki, *Phys. Rev. A* **20**, 465 (1979).
- ⁴T. Mukoyama and L. Sarkadi, *Phys. Rev. A* **23**, 375 (1981).
- ⁵T. Mukoyama and L. Sarkadi, *Phys. Rev. A* **25**, 1411 (1982).
- ⁶M. H. Chen, B. Crasemann, and H. Mark, *Phys. Rev. A* **26**, 1242 (1982).
- ⁷M. H. Chen, B. Crasemann, and H. Mark, *Phys. Rev. A* **27**, 2358 (1983).
- ⁸M. H. Chen, *Phys. Rev. A* **30**, 2082 (1984).
- ⁹M. H. Chen and B. Crasemann, *At. Data Nucl. Data Tables* **33**, 217 (1985).
- ¹⁰L. Sarkadi and T. Mukoyama, *J. Phys. B* **13**, 2255 (1980).
- ¹¹L. Sarkadi and T. Mukoyama, *J. Phys. B* **14**, L255 (1981).
- ¹²L. Sarkadi, *Nucl. Instrum. Methods* **214**, 43 (1983).
- ¹³L. Sarkadi and T. Mukoyama, *Nucl. Instrum. Methods B* **4**, 296 (1984).
- ¹⁴T. Papp, J. Pálinkás, L. Sarkadi, B. Schlenk, I. Török, and

K. Kiss, *Nucl. Instrum. Methods B* **4**, 311 (1984).

- ¹⁵J. Pálinkás, L. Sarkadi, B. Schlenk, I. Török, Gy. Kálmán, C. Bauer, K. Brankoff, D. Grambole, C. Heiser, W. Rudolph, and H. J. Thomas, *J. Phys. B* **17**, 131 (1983).
- ¹⁶L. Vegh and L. Sarkadi, *J. Phys. B* **16**, L727 (1983).
- ¹⁷W. Jitschin, A. Kaschuba, R. Hippler, and H. O. Lutz, *J. Phys. B* **15**, 763 (1982).
- ¹⁸S. Datz, J. L. Duggan, L. C. Feldman, E. Laegsgaard, and J. U. Andersen, *Phys. Rev. A* **9**, 192 (1974).
- ¹⁹W. Jitschin, G. Materlik, U. Werner, and P. Funke, *J. Phys. B* **18**, 1139 (1985).
- ²⁰M. O. Krause, *J. Phys. Chem. Ref. Data* **8**, 307 (1979).
- ²¹L. Sarkadi, *J. Phys. B* **19**, 2519 (1986).
- ²²L. Sarkadi, *J. Phys. B* **19**, L755 (1986).
- ²³J. F. Reading, *Phys. Rev. A* **8**, 3262 (1973).
- ²⁴J. H. McGuire, D. J. Land, J. G. Brennan, and G. Basbas, *Phys. Rev. A* **19**, 2180 (1979).
- ²⁵L. Sarkadi, *Nucl. Instrum. Methods* (to be published).
- ²⁶M. H. Chen, B. Crasemann, and H. Mark, *Phys. Rev. A* **24**, 177 (1981).
- ²⁷J. H. Scofield, *At. Data Nucl. Data Tables* **14**, 121 (1974).